Acta Crystallographica Section C
Crystal Structure Communications
ISSN 0108-2701

Constructor graph description of the hydrogen-bonding supramolecular assembly in two ionic compounds: 2-(pyrazol-1-yl)ethylammonium chloride and diaquadichloridobis(2-hydroxyethylammonium)cobalt(II) dichloride

Ilia A. Guzei,[a]* Lara C. Spencer,[a] Michael K. Ainooson[b] and James Darkwa[b]

[a]Department of Chemistry, University of Wisconsin–Madison, 1101 University Avenue, Madison, WI 53706, USA, and [b]Department of Chemistry, University of Johannesburg, PO Box 524, Auckland Park 2006, South Africa
Correspondence e-mail: iguzei@chem.wisc.edu

Received 8 January 2010
Accepted 11 February 2010
Online 6 March 2010

Covalent bond tables are used to generate hydrogen-bond pattern designator symbols for the crystallographically characterized title compounds. 2-(Pyrazol-1-yl)ethylammonium chloride, $C_5H_{10}N_3^+\cdot Cl^-$, (I), has three unique, strong, charge-assisted hydrogen bonds of the types N—H···Cl and N—H···N that form unary through ternary levels of graph-set interactions. Diaquadichloridobis(2-hydroxyethylammonium)-cobalt(II) dichloride, $[CoCl_2(C_2H_8NO)_2(H_2O)_2]Cl_2$, (II), forms five unique charge-assisted hydrogen bonds of the types O—H···Cl and N—H···Cl. These form graph-set patterns up to the quinary level. The Co complex in (II) resides at a crystallographic inversion center; thus the number of hydrogen bonds to consider doubles due to their *G*-equivalence, and the handling of such a case is demonstrated.

Comment

Metal ions are known to catalyze the hydrolysis of free imines (Nolan & Hay, 1974; Satchell & Satchell, 1979; Hay, 1987), although metal ions are also known to stabilize imines. Surprisingly, hydrolysis of imines is observed even when Schiff base ligands form metal complexes (Bähr & Thämlitz, 1955; Bähr & Döge, 1957). In fact, formation of imines followed by metal-assisted hydrolysis back to amines is now widely used as a way of protecting amines in organic synthesis (Deng *et al.*, 2002; Kurita, 2001; Shelley *et al.*, 1999). So why do imines hydrolyze in the presence of metal ions in some instances but generally metal ions stabilize imines? It appears counter-ions associated with the metal ion have a role to play in the hydrolysis. Recent reports by Gosh and co-workers (Chattopadhyay *et al.*, 2007) have shown that counter-ions associated with metals ions affect the hydrolysis of imines. Using nickel chloride and nickel thiocyanate they were able to show that, in the presence of strongly coordinating SCN^-, the Ni^{II} ion is unable to catalyze the hydrolysis of tetradentate Schiff base ligands, but with a weaker coordinating Cl^- ion, the Schiff base ligands hydrolyzed to the parent amine (Lee *et al.*, 1948). In spite of the apparent role counter-ions play in metal-assisted hydrolysis of imines, the Lewis acidity of the metal and the nature of the imine remain the crucial factors in determining whether a metal ion will stabilize or hydrolyze an imine. We have recently found that 4,6-di-*tert*-butyl-2-{[2-(3,5-dimethylpyrazol-1-yl)ethylimino]methyl}phenol is stabilized by $CoCl_2$ and $PdCl_2$ (Boltina *et al.*, 2010), but the unsubstituted pyrazolyl analog was hydrolyzed by $FeCl_2$, while $CoCl_2$ hydrolyzed 2-(2-hydroxyethylimino)phenol; they were hydrolyzed to the ammonium chloride compounds 2-(pyrazol-1-yl)ethylammonium chloride, (I), and diaquadichloridobis(2-hydroxyethylammonium)cobalt(II) dichloride, (II), respectively, that self-assemble *via* hydrogen bonding.

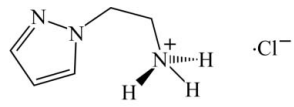

(I)

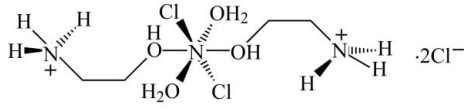

(II)

Recently, we demonstrated the application of graph-set analysis to the description of complex hydrogen-bonding interactions in the structures of (3,5-dimethyl-1*H*-pyrazol-4-ylmethyl)isopropylammonium chloride monohydrate (Guzei, Keter *et al.*, 2007) and *N*,*N*′-bis(2-hydroxy-1-methylethyl)-phthalamide (Guzei, Spencer *et al.*, 2007). In this paper, we illustrate the use of 'covalent bond tables' for the generation of the proper graph-set pattern designators. Both (I) and (II) have extensive hydrogen-bonding frameworks and provide suitable systems for studying supramolecular motifs. The 'covalent bond table' approach was originally introduced by Grell *et al.* (1999), but herein we (*a*) describe our method of generating the covalent bond table based on a diagram showing a convenient minimum number of necessary hydrogen bonds using (I) as an example, and (*b*) provide an example [compound (II)] where the symmetry-related hydrogen bonds (due to the main molecule residing on an inversion center) complicate the creation of the covalent bond table. The latter complexity arises from the crystallographic equivalence of hydrogen-bonding interactions and multiple possibilities of completing an entry in the table.

A molecular drawing of (I) is shown in Fig. 1. The bond distances and angles within the cation are typical, as confirmed by the *Mogul* structural check (Bruno *et al.*, 2004). There are three charge-assisted hydrogen-bonding interactions, denoted

a*–*c (Table 1), of two types (N—H···Cl and N—H···N). These hydrogen bonds feature rather short $D\cdots A$ distances and D—H···A angles ranging between 155.0 (14) and 161.4 (15)°, and are comparable to other similar hydrogen bonds in the Cambridge Structural Database (CSD; Version 1.11, January 2009 release; Allen, 2002).

Our procedure for generating the appropriate pattern designators for all possible hydrogen-bonding *R* (ring) and *C* (chain) patterns is based on the methodology of Grell *et al.* (1999) and involves the following steps:

(1) Assignment of a letter code to each unique bond such as ***a***, ***b***, *etc.*

(2) Creation of a molecular drawing showing all hydrogen bonds (with labels) formed by both cation and anion.

(3) Generation of the covalent bond table containing the number of covalent bonds between each pair of hydrogen bonds $\vec{a}$, $\overleftarrow{b}$, *etc*. The arrows denote the direction of the hydrogen bond: → designates a donor-to-acceptor D—H···A interaction, whereas ← represents an acceptor-to-donor A···H—D orientation.

(4) Generation of a packing diagram showing the hydrogen-bonding interactions with the letter labels ***a***, ***b***, *etc*.

(5) Identification of hydrogen-bonding motifs such as ring $R(\vec{a}\ \overleftarrow{b})$ or chain $C(\vec{c}\ \vec{d})$.

(6) Assignment of numerical values to the number of donors, acceptors and size of the pattern in the pattern designator symbol $G^{\text{acceptors}}_{\text{donors}}$(size) with the use of the covalent bond table.

The workflow for compound (I) was executed as follows. After each hydrogen bond is assigned a label (step 1, Table 1), a molecular drawing with the necessary hydrogen bonds is generated (step 2, Fig. 2). One can easily follow all possible unary and binary hydrogen-bond sequences using this drawing.

Step 3: the covalent bond table is a symmetric matrix with the dimension of twice the number of hydrogen bonds, since each bond will have two representations, for the 'forward' (*e.g.* $\vec{a}$) and 'backward' bonds (*e.g.* $\overleftarrow{a}$) (Table 2). Note that the columns list bonds in the order $\vec{a}\ \overleftarrow{a}\ \vec{b}\ \overleftarrow{b}\ \vec{c}\ \overleftarrow{c}$, whereas the rows starts with a 'backward' bond $\overleftarrow{a}\ \vec{a}\ \overleftarrow{b}\ \vec{b}\ \overleftarrow{c}\ \vec{c}$. The number of covalent bonds (or covalent edges) is now very easy to count with the help of Fig. 2. The first column is filled as follows. The number of covalent edges between bonds $\vec{a}$ (column 1) and $\overleftarrow{a}$ (row 1) is zero, since the forward bond ***a*** goes from atom H3*A* to Cl1 and the backward ***a*** bond is from Cl1 to H3*A* (there are no covalent bonds in the chloride). In generating the covalent bond table, the order in which the bonds are considered is important. When counting the covalent bonds between two hydrogen bonds, the covalent bonds are counted starting at the hydrogen bond in the column going to the hydrogen bond in the row. The second entry for bonds $\vec{a}$ (column 1) and $\vec{a}$ (row 2) is non-existent, since the forward ***a*** bond ends at Cl1 and there is no ***a*** bond originating from the chloride. The entry for bond $\vec{a}$ (column 1) and $\overleftarrow{b}$ (row 3) is absent because there are no covalent bonds between bonds N3—H3*A*···Cl1 ($\vec{a}$) and N1···H3*B*—N3 ($\overleftarrow{b}$). The $\vec{a}\ \vec{b}$ entry is also absent, the entry for bond $\vec{a}$ (column 1) and $\overleftarrow{c}$ (row 5) is again zero because the bonds meet at the chloride, and the $\vec{a}\ \overleftarrow{c}$ entry is absent. The table is symmetric;

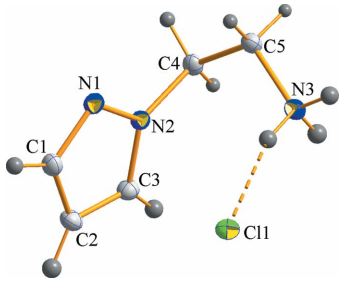

Figure 1
A molecular diagram of (I) shown with 50% probability ellipsoids. The dashed line represents a hydrogen-bonding interaction.

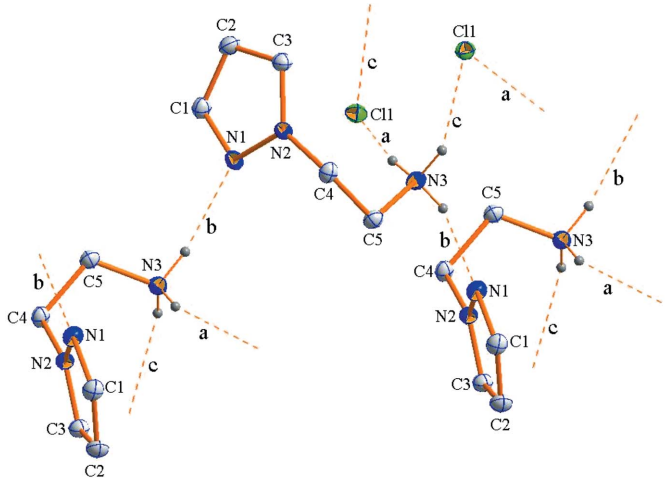

Figure 2
A diagram of (I) shown with 50% probability ellipsoids and with the convenient minimum number of hydrogen bonds to generate the covalent bond table.

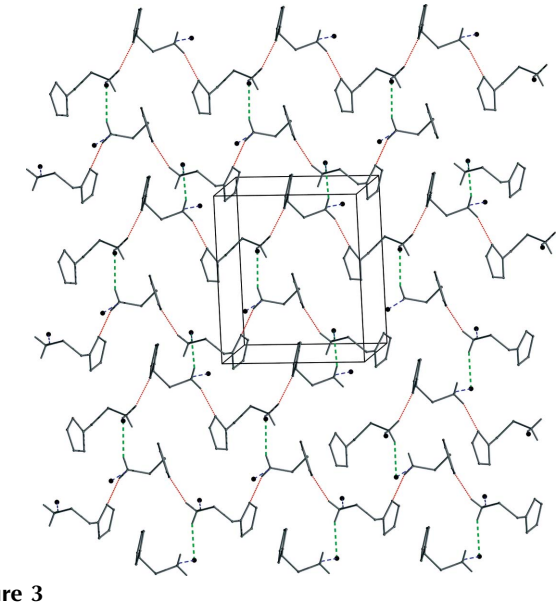

Figure 3
A packing diagram of (I) viewed along the *a* axis. Hydrogen bonds are coded as follows: ***a***, blue, three-dash diagonal line; ***b***, red, near-vertical dotted line; ***c***, green, vertical dashed line.

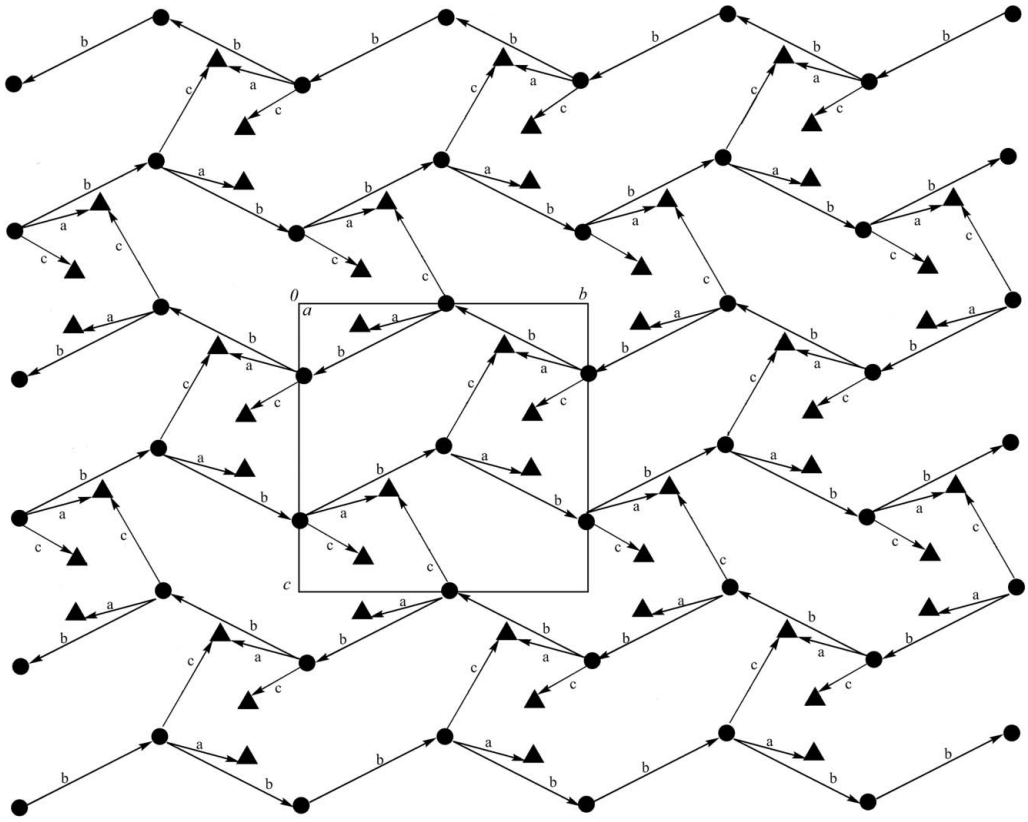

Figure 4
A constructor graph representation of (I), viewed along the *a* axis. Circles denote the cations and triangles denote the chloride anions. Arrows point from the donor to the acceptor.

thus the first row contains the same entries as the first column. The second column corresponding to $\overleftarrow{\boldsymbol{a}}$ contains more numerical entries. The first entry corresponding to $\overleftarrow{\boldsymbol{a}}\,\overleftarrow{\boldsymbol{a}}$ is non-existent, the second cell corresponding to $\overleftarrow{\boldsymbol{a}}\,\overrightarrow{\boldsymbol{a}}$ is zero. The third cell shows the number of covalent bonds between bond $\overleftarrow{\boldsymbol{a}}$ (column 2) and bond $\overleftarrow{\boldsymbol{b}}$ (row 3) – there are five bonds, namely H3*A*—N3, N3—C5, C5—C4, C4—N2 and N2—N1. The fourth cell in column 2 corresponds to $\overleftarrow{\boldsymbol{a}}\,\overrightarrow{\boldsymbol{b}}$ and the number of covalent bonds between atoms H3*A* and H3*B* is two. The fifth cell (entry is non-existent) represents the covalent bond count in the sequence $\overleftarrow{\boldsymbol{a}}\,\overleftarrow{\boldsymbol{c}}$. The last entry $\overleftarrow{\boldsymbol{a}}\,\overrightarrow{\boldsymbol{c}}$ is the number of covalent bonds between H3*A* and H3*C*, which is two. The second row is identical to the second column. The rest of the table is filled out in a similar fashion.

Step 4: the packing diagram showing the color-coded hydrogen bonds is presented in Fig. 3. To facilitate the hydrogen-bonding pattern identification it may be easier to eliminate all the covalent edges from the drawing in order to depict all the interactions schematically (Fig. 4).

Step 5: an examination of projections along the *a* and *b* axes clearly reveals that the cations are linked into chains $C(\overrightarrow{\boldsymbol{b}})$ in the crystallographic *b* direction (Fig. 5) and cations and anions alternately into zigzag chains $C(\overrightarrow{\boldsymbol{a}}\,\overleftarrow{\boldsymbol{c}})$ in the crystallographic *a* direction (Fig. 6). These zigzag rows of alternating ***a*** and ***c*** hydrogen bonds are connected by the ***b*** hydrogen bond to form two-dimensional sheets.

Step 6: the designators pattern symbol $G^{\text{acceptors}}_{\text{donors}}(\text{size})$ is generated. The covalent bond table was created specifically for this step. Chains $C(\overrightarrow{\boldsymbol{b}})$ are formed by ***b*** bonds only (Fig. 5); therefore the number of donors and acceptors is one apiece. The full symbol would thus be $C^1_1(\text{size})$, but one donor and one acceptor are the default values not explicitly written in the designator. The size of the pattern corresponds to the $\overrightarrow{\boldsymbol{b}}\,\overrightarrow{\boldsymbol{b}}$ entry in the covalent bond table (5) plus the number of hydrogen bonds the pattern involves (1). Thus, the correct

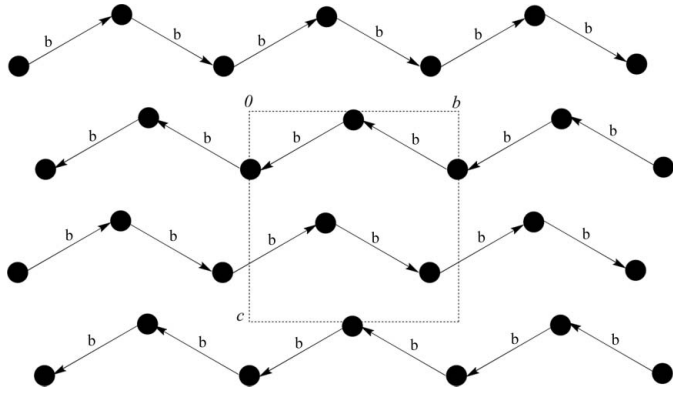

Figure 5
A constructor graph projection of the hydrogen-bonding interaction ***b*** of (I) along the *a* axis. Circles denote the cations. Arrows point from the donor to the acceptor.

pattern designator for the primary-level chain $C(\vec{b})$ is $C_1^1(6)$, or simply $C(6)$.

For the pattern $C(\vec{a}\,\overleftarrow{c})$ (Fig. 6), two entries from the covalent bond table are necessary, corresponding to $\vec{a}\,\overleftarrow{c}$ (0), and to $\overleftarrow{c}\,\vec{a}$ (2) because the pattern repeats. There are two hydrogen bonds involved; therefore the size is 0 + 2 + 2 = 4. There are two hydrogen bonds, and therefore two donors (for exceptions, see Grell *et al.*, 1999). The number of acceptors is the number of bonds minus the number of arrows in the pattern pointing toward each other (meaning there is only one acceptor involved). In the pattern $\vec{a}\,\overleftarrow{c}$ in question, the two arrows point toward each other, hence the number of acceptors is 2 − 1 = 1. Consequently, the pattern designator for a secondary-level chain $C(\vec{a}\,\overleftarrow{c})$ is $C_2^1(7)$. These results could also be obtained by visual inspection, but our approach is substantially less error prone.

Since this system features three types of hydrogen bonds it is possible to construct ternary systems, such as chain $C(\vec{c}\,\overleftarrow{a}\,\overleftarrow{b})$ and ring $R(\vec{a}\,\overleftarrow{c}\,\overleftarrow{b}\,\vec{b}\,\vec{c}\,\overleftarrow{a}\,\overleftarrow{b}\,\overleftarrow{b})$. The covalent bond table makes generation of the designator pattern symbol $G_{\text{donors}}^{\text{acceptors}}(\text{size})$ a trivial exercise. For $C(\vec{c}\,\overleftarrow{a}\,\overleftarrow{b})$ we have three donors, two acceptors (two arrows point toward each other), and the size is 0 ($\vec{c}\,\overleftarrow{a}$ table entry) + 5 ($\overleftarrow{a}\,\overleftarrow{b}$ table entry) + 2 ($\overleftarrow{b}\,\vec{c}$ table entry) + 3 (number of hydrogen bonds) = 10. Thus, the symbol for the $C(\vec{c}\,\overleftarrow{a}\,\overleftarrow{b})$ chain is $C_3^2(10)$. Similarly, for ring $R(\vec{a}\,\overleftarrow{c}\,\overleftarrow{b}\,\vec{b}\,\vec{c}\,\overleftarrow{a}\,\overleftarrow{b}\,\overleftarrow{b})$ one obtains $R_8^6(32)$. In this case, the size is determined as the sum of 0 + 5 + 5 + 2 + 0 + 5 + 5 + 2 + 8 (number of hydrogen bonds) = 32. The program *Mercury* (Bruno *et al.*, 2002) now has an option for conveniently calculating graph sets, but it may not generate a symbol for a particular pattern one is interested in.

Compound (II) crystallizes in the centrosymmetric triclinic space group $P\overline{1}$. The cation occupies a crystallographic inversion center (Fig. 7). The bond distances and angles within the cation are unexceptional (Table 3), as confirmed by the *Mogul* structural check. There are five strong charge-assisted hydrogen-bonding interactions, denoted ***a*–*e*** (Table 4), of two types (O—H···Cl and N—H···Cl). These hydrogen bonds feature rather short $D\cdots A$ distances and D—H$\cdots A$ angles spanning the range 152.2 (17)–171.3 (18)°, and are comparable to other similar hydrogen bonds in the CSD. Thus, each cation acts as a donor in ten hydrogen bonds and an acceptor in two, while each chloride anion acts as an acceptor in four hydrogen bonds.

The structure of the ionic compound presented us with an interesting dilemma. As a result of the large number of acidic H atoms (six in the asymmetric unit) and hydrogen-bond acceptors, one of which is formally negatively charged (Cl2), we had to evaluate the significance of each possible hydrogen-bonding interaction (Table 4). The bonds can be classified as 'classic' bifurcated and trifurcated. There are six classic hydrogen bonds, but only five satisfy the usual criterion of direction (D—H$\cdots A$ angle between 150 and 180°). The other bond is clearly outside the range of D—H$\cdots A$ angles considered acceptable for strong classic hydrogen bonds (*vide infra*, Step 4).

Our graph-set analysis will follow the previously outlined six steps. The results of step 1, assignment of a letter code to each type of bond, are presented in Table 4.

Step 2, preparation of a molecular drawing showing all hydrogen bonds, is accomplished with Fig. 8. The cation occupies a crystallographic inversion center; therefore each hydrogen bond has a symmetry-related counterpart. Hydrogen bonds related by inversion are *G*-equivalent, in the sense that a symmetry transformation *g* in the space group *G* will map one bond onto the other. This will present ambiguities when graph-set notations are generated because it would be possible to select paths with the same bond-label sequences but with a different number of bonds. To avoid these ambiguities, all *G*-equivalent bonds are also assigned a number; thus bond ***a*1** is related by inversion to ***a*2**, ***b*1** is related by inversion to ***b*2**, *etc.* Hydrogen bonds related by

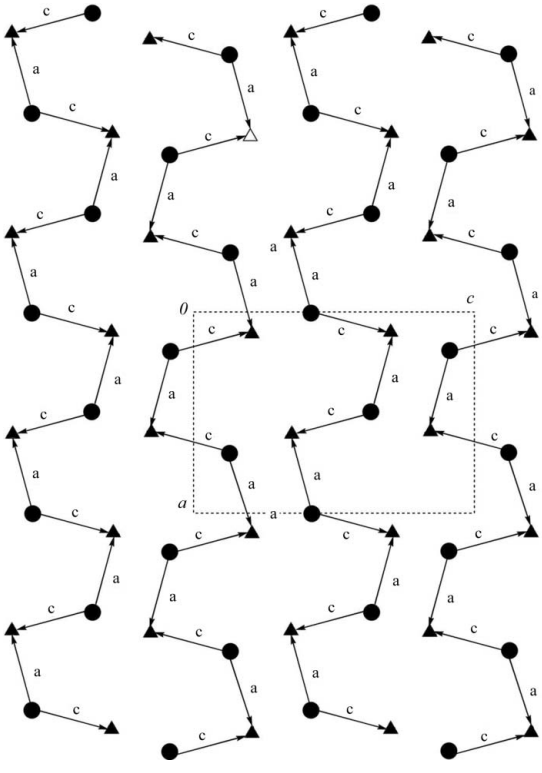

Figure 6
A constructor graph projection of the hydrogen-bonding interactions ***a*** and ***c*** of (I) on to the *ac* plane. Circles denote the cations and triangles denote the chloride anions. Arrows point from the donor to the acceptor.

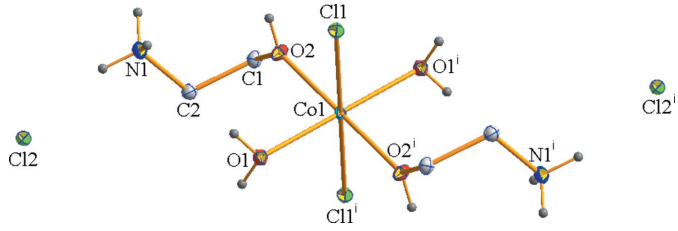

Figure 7
A molecular diagram of (II) shown with 50% probability ellipsoids. All H atoms residing on C atoms have been omitted for clarity. [Symmetry code: (i) $-x-2, -y+2, -z+2$.]

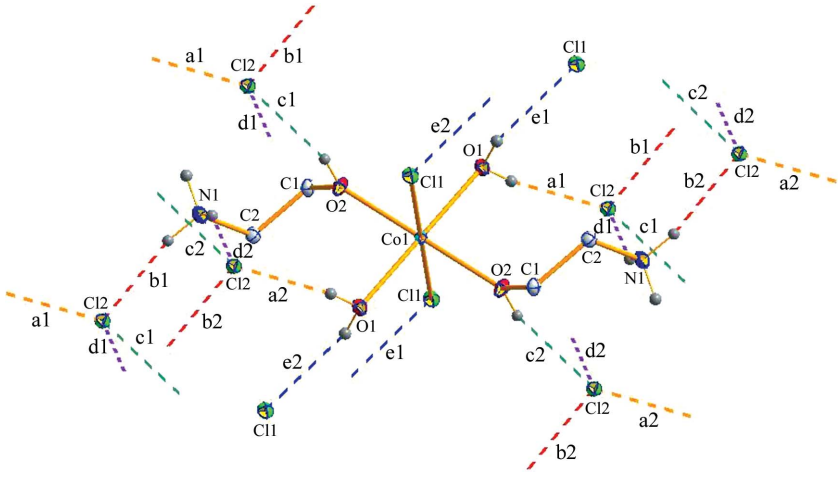

Figure 8
A diagram of (II) shown with 50% probability ellipsoids and with a convenient minimum number of hydrogen bonds to generate the covalent bond table. All H atoms connected to C atoms have been omitted for clarity.

translation are *T*-equivalent and have the same letter codes in Fig. 8.

Step 3 involves the creation of the covalent bond table. This procedure is moderately labor intensive because of the presence of five hydrogen bonds and their *G*-equivalents, and we generate entries both for 'forward' and 'backward' bonds. The table dimensions are 20 × 20, but all diagonal elements are zeros and the symmetry of the table reduces the number of entries we must generate by half, which means that instead of 400 values only 190 have to be tabulated. Table 5 is the outcome of our visual inspection of Fig. 8.

Step 4: the strong hydrogen-bonding interactions link the ions into two-dimensional sheets in the *ac* plane (Fig. 9). The sheets are then stacked along the *b* axis (Fig. 10). The sheets are linked by a hydrogen-bonding interaction, N1—H1*E*···Cl2, with a donor-to-acceptor distance of 3.3815 (18) Å, which is considered to be weak because of the suboptimal N1—H1···Cl2 angle of 140.5 (15)°. This weak interaction was not included in the constructor graph and graph-set analysis that follows.

Steps 5 and 6: the hydrogen-bonding interaction network in (II) can be readily visualized with the help of the constructor graph (Fig. 11). Unary-level patterns (those formed with one type of hydrogen bond) include the chain $C(\overrightarrow{\boldsymbol{e}})$ equivalent to chains $C(\overrightarrow{\boldsymbol{e1}})$ and $C(\overrightarrow{\boldsymbol{e2}})$. The size of this $C(\overrightarrow{\boldsymbol{e}})$ pattern is 3 (the $\overrightarrow{\boldsymbol{e1}}\,\overrightarrow{\boldsymbol{e1}}$ entry in Table 5) + 1 (number of hydrogen bonds) = 4. Thus, the pattern designator symbol is $C(4)$. Another unary pattern, ring $R(\overrightarrow{\boldsymbol{e1}}\,\overrightarrow{\boldsymbol{e2}})$, has a size of 3 + 3 + 2 = 8 and the full symbol of $R_2^2(8)$.

Binary-level patterns include the chain $C(\overrightarrow{\boldsymbol{b1}}\overleftarrow{\boldsymbol{c1}})$ and the ring $R(\overrightarrow{\boldsymbol{a1}}\overleftarrow{\boldsymbol{d1}})$. The number of hydrogen donors in each pattern is 2, but the number of acceptors is 1 (the arrows in the

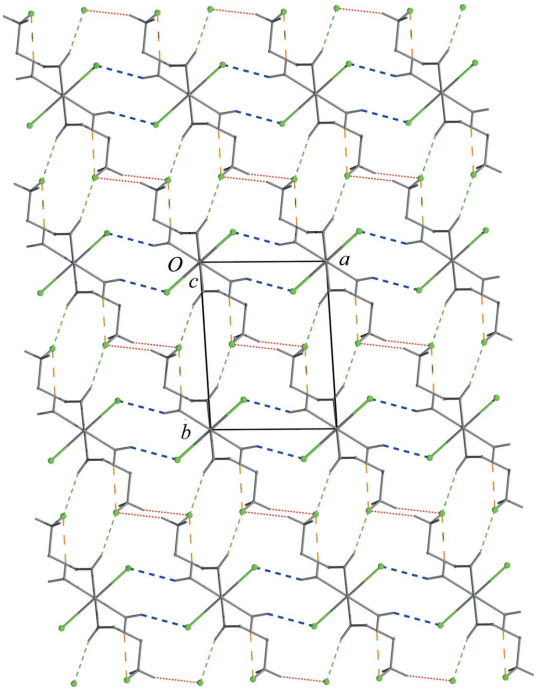

Figure 9
A packing diagram of (II) viewed along the *b* axis. Two-dimensional sheets are formed by the strong hydrogen bonds, ***a***–***e***. The hydrogen bonds are coded as follows: ***a***, orange, vertical three-dash line; ***b***, red, horizontal dotted line; ***c***, green, vertical five-dash line; ***d***, purple, not visible; ***e***, blue, horizontal five-dash line.

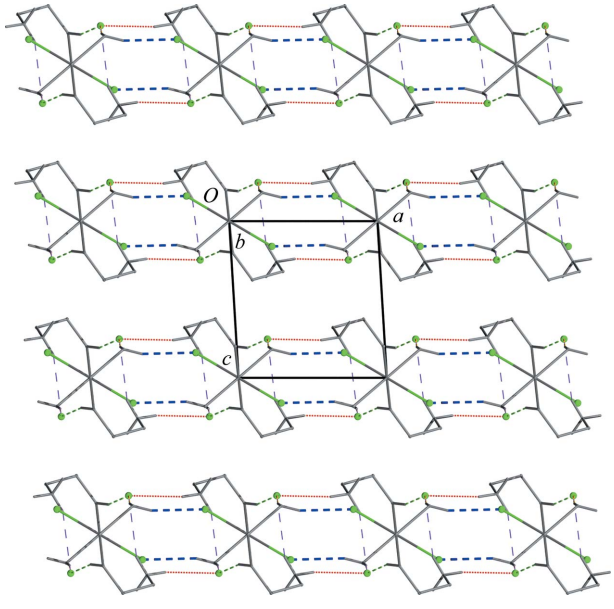

Figure 10
A packing diagram of (II) viewed along the *c* axis. Two-dimensional sheets are stacked along the *b* axis. The hydrogen bonds are coded as follows: ***a***, orange, not clearly visible; ***b***, red, horizontal dotted line; ***c***, green, vertical three-dash line; ***d***, purple, vertical three-dash line; ***e***, blue, horizontal five-dash line.

patterns point head-to-head, and involve a Cl^- anion that is the acceptor of both bonds). The covalent bond table is used for facile pattern size determination. For $C(\overrightarrow{b1}\overleftarrow{c1})$ it is the sum of 0 ($\overrightarrow{b1}\overleftarrow{c1}$ entry in the table) + 5 ($\overleftarrow{c1}\overrightarrow{b1}$ entry in the table) + 2 (number of hydrogen bonds) = 7, resulting in the $C_2^1(7)$ designator. Similarly, rings $R(\overrightarrow{a1}\overleftarrow{d1})$ are described with $R_2^1(9)$.

Ternary patterns are exemplified by the chain $C(\overrightarrow{a1}\overleftarrow{b1}\overrightarrow{d1}\overleftarrow{b1})$ and the ring $R(\overrightarrow{b2}\overrightarrow{c2}\overleftarrow{e1})$. The chain pattern has four donors but two (4 − 2 = 2) acceptors with the size of 0 + 10 + 0 + 7 + 4 = 21. This patterns is described with $C_4^2(21)$. The ring pattern is created with three donors but two acceptors and its size computed by summation of four terms 0 + 4 + 6 + 3 = 13. Thus, the pattern designator is $R_3^2(13)$.

A quaternary zigzag chain pattern is identified with the sequence $\overrightarrow{a1}\overleftarrow{b1}\overrightarrow{d2}\overleftarrow{c2}$. There are four donors, two acceptors (4 − 2 = 2), and the size is 10 (0 + 2 + 0 + 4 + 4) for the pattern designator $C_4^2(10)$.

An obvious quinary-level pattern is ring $\overrightarrow{a1}\overleftarrow{c1}\overrightarrow{e2}\overrightarrow{d2}\overleftarrow{b2}$. It involves two chloride anions (and there are two occurrences of arrows pointing head-to-head); thus there are three acceptors for the five donors, and the size is 0 + 4 + 6 + 0 + 7 + 5 = 22. The pattern designator is $R_5^3(22)$.

Note that the currently used pattern designators do not allow for the inclusion of the pattern-level value in its symbol.

Compounds (I) and (II) have unexceptional molecular geometries but form interesting two- and three-dimensional supramolecular structures as a result of hydrogen-bonding interactions. We have explained and demonstrated the use of covalent bond tables and constructor graph diagrams for identification and classification of hydrogen-bonding pattern designators. These compounds provide examples of the usefulness of such tools and the need for their mainstream use in crystallography.

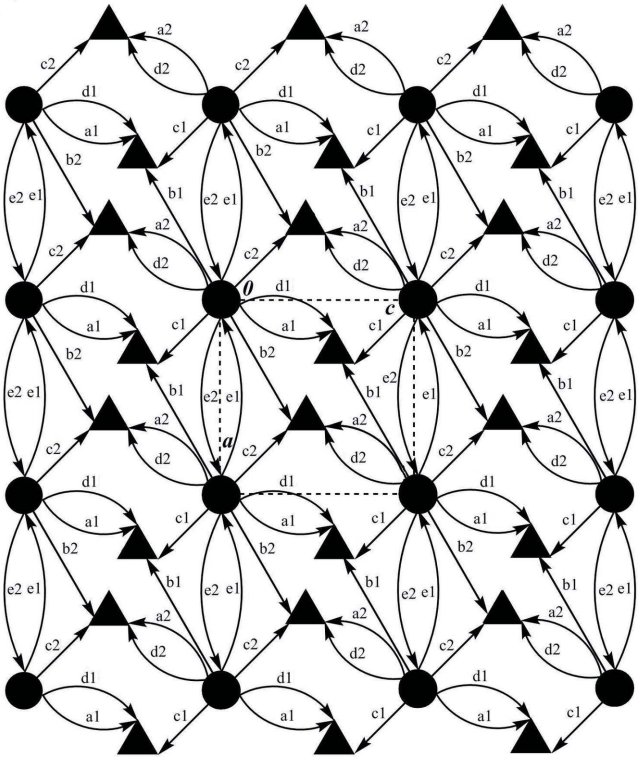

Figure 11
A constructor graph representation of (II) viewed along the *b* axis. Circles denote the cations and triangles denote the chloride anions. Arrows point from the donor to the acceptor. The bonds with index 2 are *G*-equivalents of bonds with index 1.

Experimental

For the synthesis of (I), $FeCl_2$ (0.051 g, 0.40 mmol) was added to a solution of *L*1 {4,6-di-*tert*-butyl-2-[2-(pyrazol-1-yl)ethylimino]-phenol} (0.26 g, 0.80 mmol) in CH_2Cl_2 (20 ml). The resulting solution was stirred for 18 h under nitrogen, after which the reaction mixture was filtered and the filtrate concentrated to about 10 ml. Subsequent addition of an equal volume of hexane precipitated a dark-green powdery paramagnetic material. A CH_2Cl_2 solution of this material slowly produced colorless crystals of (I) over several days, while the bulk of the solution remained green.

For the synthesis of (II), a solution of *L*2 [2-(hydroxyethylimino)phenol] (0.50 g, 3.00 mmol) and $CoCl_2$ (0.39 g, 3.00 mmol) in tetrahydrofuran (15 ml) was stirred at room temperature for 24 h, resulting in a dark-green solution. After concentrating the solution to half its volume and adding about 10 ml of hexane, a dark-green solid precipitated. This material was re-dissolved in CH_2Cl_2, layered with hexane and left for about a week during which time purple crystals of compound (II) formed while the bulk of the solution remained green.

Compound (I)

Crystal data

$C_5H_{10}N_3^+\cdot Cl^-$
M_r = 147.61
Orthorhombic, $P2_12_12_1$
a = 6.9634 (11) Å
b = 9.3732 (14) Å
c = 10.9416 (17) Å
V = 714.15 (19) Å^3
Z = 4
Mo *K*α radiation
μ = 0.45 mm^{-1}
T = 100 K
0.45 × 0.27 × 0.11 mm

Data collection

Bruker CCD 1000 area-detector diffractometer
Absorption correction: multi-scan (*SADABS*; Bruker, 2007)
T_{min} = 0.824, T_{max} = 0.952
10559 measured reflections
2035 independent reflections
1991 reflections with $I > 2\sigma(I)$
R_{int} = 0.026

Refinement

$R[F^2 > 2\sigma(F^2)]$ = 0.022
$wR(F^2)$ = 0.060
S = 1.07
2035 reflections
123 parameters
All H-atom parameters refined
$\Delta\rho_{max}$ = 0.36 e Å^{-3}
$\Delta\rho_{min}$ = −0.14 e Å^{-3}
Absolute structure: Flack (1983)
Flack parameter: −0.01 (4)

Table 1
Strong hydrogen-bonding interactions in (I).

Label	*D*—H···*A*	*D*—H	H···*A*	*D*···*A*	*D*—H···*A*
a	N3—H3*A*···Cl1	0.812 (17)	2.323 (17)	3.1003 (11)	160.4 (15)
b	N3—H3*B*···N1^{i}	0.879 (17)	2.046 (18)	2.8920 (13)	161.4 (15)
c	N3—H3*C*···Cl1^{ii}	0.864 (19)	2.348 (19)	3.1522 (11)	155.0 (14)

Symmetry codes: (i) $-x+1, y+\frac{1}{2}, -z+\frac{1}{2}$; (ii) $x-\frac{1}{2}, -y+\frac{3}{2}, -z$.

Table 2
Covalent bond table for (I).

	$\vec{a}$	$\overleftarrow{a}$	$\vec{b}$	$\overleftarrow{b}$	$\vec{c}$	$\overleftarrow{c}$
$\overleftarrow{a}$	0	–	–	–	0	–
$\vec{a}$	–	0	5	2	–	2
$\overleftarrow{b}$	–	5	0	5	–	5
$\vec{b}$	–	2	5	0	–	2
$\overleftarrow{c}$	0	–	–	–	0	–
$\vec{c}$	–	2	5	2	–	0

Table 3
Selected geometric parameters (Å, °) for (II).

Co1—O1	2.0683 (12)	Co1—Cl1	2.4400 (12)
Co1—O2	2.0852 (11)		
O1—Co1—O2^{i}	91.51 (5)	O2—Co1—Cl1^{i}	94.14 (4)
O1—Co1—O2	88.49 (5)	O1—Co1—Cl1	90.83 (4)
O1—Co1—Cl1^{i}	89.17 (4)	O2—Co1—Cl1	85.86 (4)

Symmetry code: (i) $-x+2, -y+2, -z+2$.

Table 4
Strong hydrogen-bonding interactions in (II).

Label	D—H$\cdots A$	D—H	H$\cdots A$	$D\cdots A$	D—H$\cdots A$
a	O1—H1$A\cdots$Cl2^{i}	0.77 (2)	2.34 (2)	3.1094 (14)	171.3 (18)
b	N1—H1$F\cdots$Cl2	0.860 (19)	2.313 (19)	3.1360 (15)	160.3 (16)
c	O2—H2$\cdots$Cl2^{ii}	0.805 (19)	2.329 (19)	3.0884 (16)	157.6 (17)
d	N1—H1$D\cdots$Cl2^{i}	0.883 (19)	2.608 (19)	3.4349 (19)	156.4 (15)
e	O1—H1$B\cdots$Cl1^{iii}	0.81 (2)	2.39 (2)	3.1315 (14)	152.2 (17)

Symmetry codes: (i) $-x+1, -y+2, -z+1$; (ii) $x+1, y, z$; (iii) $x-1, y, z$.

Compound (II)

Crystal data

$[CoCl_2(C_2H_8NO)_2(H_2O)_2]Cl_2$
M_r = 360.95
Triclinic, $P\overline{1}$
a = 6.258 (2) Å
b = 6.653 (3) Å
c = 8.369 (3) Å
α = 83.57 (3)°
β = 86.37 (5)°
γ = 86.19 (2)°
V = 344.9 (2) Å^3
Z = 1
Mo $K\alpha$ radiation
μ = 2.02 mm^{-1}
T = 100 K
0.43 × 0.29 × 0.14 mm

Data collection

Bruker CCD 1000 area-detector diffractometer
Absorption correction: multi-scan (*SADABS*; Bruker, 2007)
T_{min} = 0.478, T_{max} = 0.766
4432 measured reflections
1560 independent reflections
1555 reflections with $I > 2\sigma(I)$
R_{int} = 0.021

Refinement

$R[F^2 > 2\sigma(F^2)]$ = 0.018
$wR(F^2)$ = 0.047
S = 1.04
1560 reflections
110 parameters
All H-atom parameters refined
$\Delta\rho_{max}$ = 0.33 e Å^{-3}
$\Delta\rho_{min}$ = −0.46 e Å^{-3}

All H atoms were placed in idealized locations and refined as riding with appropriate displacement parameters, U_{iso}(H) = 1.2 or 1.5U_{eq}(parent atom). The outlier reflections were omitted based on the statistics test described in Prince & Nicholson (1983) and Rollett (1988), and implemented in program *FCF_filter* (Guzei, 2007); the number of omitted outliers is 2 for (I) and 4 for (II).

Table 5
Covalent bond table for (II).

	$\vec{a1}$	$\overleftarrow{a1}$	$\vec{a2}$	$\overleftarrow{a2}$	$\vec{b1}$	$\overleftarrow{b1}$	$\vec{b2}$	$\overleftarrow{b2}$	$\vec{c1}$	$\overleftarrow{c1}$	$\vec{c2}$	$\overleftarrow{c2}$	$\vec{d1}$	$\overleftarrow{d1}$	$\vec{d2}$	$\overleftarrow{d2}$	$\vec{e1}$	$\overleftarrow{e1}$	$\vec{e2}$	$\overleftarrow{e2}$
$\overleftarrow{a1}$	0	–	–	–	0	–	–	–	0	–	–	–	0	–	–	–	–	–	–	–
$\vec{a1}$	–	0	–	4	–	7	–	7	–	4	–	4	–	7	–	7	3	2	3	4
$\overleftarrow{a2}$	–	–	0	–	–	–	0	–	–	–	0	–	–	–	0	–	–	–	–	–
$\vec{a2}$	–	4	–	0	–	7	–	7	–	4	–	4	–	7	–	7	3	4	3	2
$\overleftarrow{b1}$	0	–	–	–	0	–	–	–	0	–	–	–	0	–	–	–	–	–	–	–
$\vec{b1}$	–	7	–	7	–	0	–	10	–	5	–	7	–	10	–	2	6	7	6	7
$\overleftarrow{b2}$	–	–	0	–	–	–	0	–	–	–	0	–	–	–	0	–	–	–	–	–
$\vec{b2}$	–	7	–	7	–	10	–	0	–	7	–	5	–	2	–	10	6	7	6	7
$\overleftarrow{c1}$	0	–	–	–	0	–	–	–	0	–	–	–	0	–	–	–	–	–	–	–
$\vec{c1}$	–	4	–	4	–	5	–	7	–	0	–	4	–	7	–	5	3	4	3	4
$\overleftarrow{c2}$	–	–	0	–	–	–	0	–	–	–	0	–	–	–	0	–	–	–	–	–
$\vec{c2}$	–	4	–	4	–	7	–	5	–	4	–	0	–	5	–	7	3	4	3	4
$\overleftarrow{d1}$	0	–	–	–	0	–	–	–	0	–	–	–	0	–	–	–	–	–	–	–
$\vec{d1}$	–	7	–	7	–	10	–	2	–	7	–	5	–	0	–	10	6	7	6	7
$\overleftarrow{d2}$	–	–	0	–	–	–	0	–	–	–	0	–	–	–	0	–	–	–	–	–
$\vec{d2}$	–	7	–	7	–	2	–	10	–	5	–	7	–	10	–	0	6	7	6	7
$\overleftarrow{e1}$	–	3	–	3	–	6	–	6	–	3	–	3	–	6	–	6	0	3	2	3
$\vec{e1}$	–	2	–	4	–	7	–	7	–	4	–	4	–	7	–	7	3	0	3	4
$\overleftarrow{e2}$	–	3	–	3	–	6	–	6	–	3	–	3	–	6	–	6	2	3	0	3
$\vec{e2}$	–	4	–	2	–	7	–	7	–	4	–	4	–	7	–	7	3	4	3	0

For both compounds, data collection: *SMART* (Bruker, 2000); cell refinement: *SAINT* (Bruker, 2007); data reduction: *SAINT*; program(s) used to solve structure: *SHELXTL* (Sheldrick, 2008); program(s) used to refine structure: *SHELXTL*; molecular graphics: *SHELXTL* and *DIAMOND* (Brandenburg, 2007); software used to prepare material for publication: *SHELXTL*, *modiCIFer* (Guzei, 2007) and *publCIF* (Westrip, 2010).

Financial support for this work from the National Research Foundation (South Africa) and the University of Johannesburg (South Africa) is gratefully acknowledged.

Supplementary data for this paper are available from the IUCr electronic archives (Reference: KU3022). Services for accessing these data are described at the back of the journal.

References

Allen, F. H. (2002). *Acta Cryst.* B**58**, 380–388.
Bähr, G. & Döge, H.-G. (1957). *Z. Anorg. Allg. Chem.* **292**, 119–138.
Bähr, G. & Thämlitz, H. (1955). *Z. Anorg. Allg. Chem.* **282**, 3–11.
Boltina, S., Ainooson, M. J., Guzei, I. A. & Darkwa, J. (2010). Unpublished results.
Brandenburg, K. (2007). *DIAMOND*. Crystal Impact GbR, Bonn, Germany.
Bruker (2000). *SMART*. Bruker AXS Inc., Madison, Wisconsin, USA.
Bruker (2007). *SADABS* and *SAINT*. Bruker AXS Inc., Madison, Wisconsin, USA.
Bruno, I. J., Cole, J. C., Edgington, P. R., Kessler, M., Macrae, C. F., McCabe, P., Pearson, J. & Taylor, R. (2002). *Acta Cryst.* B**58**, 389–397.
Bruno, I. J., Cole, J. C., Kessler, M., Luo, J., Motherwell, W. D. S., Purkis, L. H., Smith, B. R., Taylor, R., Cooper, R. I., Harris, S. E. & Orpen, A. G. (2004). *J. Chem. Inf. Comput. Sci.* **44**, 2133–2144.
Chattopadhyay, S., Brew, M. D. G. & Gosh, A. (2007). *Polyhedron*, **26**, 3513–3522.
Deng, W.-P., Wong, K. A. & Kirk, K. L. (2002). *Tetrahedron Asymmetry*, **13**, 1135–1140.
Flack, H. D. (1983). *Acta Cryst.* A**39**, 876–881.
Grell, J., Bernstein, J. & Tinhofer, G. (1999). *Acta Cryst.* B**55**, 1030–1043.
Guzei, I. A. (2007). In-house Crystallographic Programs, Molecular Structure Laboratory, University of Wisconsin–Madison, Madison, Wisconsin, USA.
Guzei, I. A., Keter, F. K., Spencer, L. C. & Darkwa, J. (2007). *Acta Cryst.* C**63**, o481–o483.

Guzei, I. A., Spencer, L. C., McGaff, R. W., Kieler, H. M. & Robinson, J. R. (2007). *Acta Cryst.* C**63**, o255–o258.
Hay, R. W. (1987). In *Comprehensive Chemistry*. Oxford: Pergamon.
Kurita, K. (2001). *Prog. Polym. Sci.* **26**, 1921–1971.
Lee, T. S., Kolthoff, I. M. & Leussing, D. L. (1948). *J. Am. Chem. Soc.* **70**, 3596–3600.
Nolan, K. B. & Hay, R. W. (1974). *J. Chem. Soc. Dalton Trans.* pp. 914–920.
Prince, E. & Nicholson, W. L. (1983). *Acta Cryst.* A**39**, 407–410.
Rollett, J. S. (1988). *Crystallographic Computing 4*, pp. 149–166. Oxford University Press.
Satchell, D. P. N. & Satchell, R. S. (1979). *Annu. Rep. Chem. Sect. A Inorg. Chem.* **75**, 25–48.
Sheldrick, G. M. (2008). *Acta Cryst.* A**64**, 112–122.
Shelley, M. D., Hartley, L., Fish, R. G., Groundwater, P., Morgan, J. J. G., Mort, D., Mason, M. & Evans, A. (1999). *Cancer Lett.* **135**, 171–180.
Westrip, S. P. (2010). *publCIF*. In preparation.